

TMD effectiveness in nonlinear RC structures subjected to near fault earthquakes

Martin N. Domizio^{1,2a}, Daniel Ambrosini^{*1,2} and Oscar Curadelli^{1,2b}

¹Faculty of Engineering, National University of Cuyo, Mendoza, Argentina
²CONICET, National Research Council, Argentina

(Received March 8, 2019, Revised July 6, 2019, Accepted July 25, 2019)

Abstract. The use of Tuned mass dampers (TMD) has proved to be effective in reducing the effects of vibrations caused by wind loads and far-field seismic action. However, its effectiveness in controlling the dynamic response of structures under near-fault earthquakes is still under discussion. In this case, the uncertainty about the TMD performance arises from the short significant duration of near-fault ground motions. In this work, the TMD effectiveness for increasing the safety margin against collapse of structures subjected to near-fault earthquakes is investigated. In order to evaluate the TMD performance in the proposed scenario, the nonlinear dynamic response of two reinforced concrete (RC) frames was analyzed. TMDs with different mass values were added to these structures, and a set of near-fault records with frequency content close to the fundamental frequency of the structure was employed. Through a series of nonlinear dynamic analysis, the minimum amplitude of each seismic record that causes the structural collapse was found. By comparing this value, called collapse acceleration, for the case of the structures with and without TMD, the benefit produced by the addition of the control device was established.

Keywords: tuned mass damper; seismic action; near-fault earthquakes; reinforced concrete structures

1. Introduction

Tuned mass dampers (TMD) are devices used to reduce vibrations in various fields of engineering. In its most basic form, these devices are composed of a mass connected to the main structure by a spring. Relative oscillation between the TMD mass and the structure to be protected produces an energy transfer from the main structure to the control device. This energy transfer reaches a maximum when the relative oscillation frequency is close to the frequency of the mode to be controlled.

In order to control the seismic response of civil structures, many passive energy dissipation devices has been studied and proposed in the last decades (Losanno *et al.* 2017, Hsiao *et al.* 2016, Choi *et al.* 2017, Shen *et al.* 2017, Cheng and Chen 2014). TMDs have been employed in vibration control since the early twentieth century, but its specific application in civil structures is more recent. Several authors have performed both numerical and experimental studies on the use of TMDs to control the structural response against seismic and wind loads (Yu *et al.* 2010, Rakicevic *et al.* 2012, Jiang *et al.* 2014, Niu *et al.* 2018), as well on the optimization of the parameters that define their behavior (Greco *et al.* 2014, Hoang *et al.* 2016, Miranda 2013, Salvi and Rizzi 2016, Jimenez-Alonso and Saez 2018) and alternatives to classical arrangement to improve its performance (Lin *et al.* 2015, Pisal and Jangid 2016, Daniel

and Lavan 2013, Lu *et al.* 2016). Elias *et al.* (2017) studied the use of multiple TMDs in order to control the response of a structure under seismic action. The authors proposed to tune TMDs with the frequency of five vibration modes and to install these devices in the antinodes of each mode. This approach proved to be more efficient and robust compared to other traditional strategies in the use of TMDs. Engle *et al.* (2015) proposed the implementation of TMDs with a large amount of mass through the isolation of floor slabs with curved surface sliders (CSSs). By means of the proposed method, it was shown that it is possible to reduce the inter-story drift up to 45% compared to the case without control. Lu *et al.* (2017) studied experimentally and analytically the performance of a particle TMD. In this case, the TMD mass consists of steel balls installed inside a box and the control device dissipates energy as a particle damper. The device was tuned with the first mode of the structure to be protected and it proved to be effective under seismic loading, with a robust behavior since it has a wide bandwidth of suppressed frequencies. Fadel Miguel *et al.* (2016) optimized the location and dynamic parameters of multiple TMDs (MTMD) in order to control the structural response under seismic excitation. The optimization was achieved using a hybrid scheme, which starts with a firefly algorithm and ends with a Nelder-Mead algorithm. In the analyzed example of a 10-story building, the optimum proved to be multiple non-uniform TMDs located on the top floor.

In contrast to long distance earthquakes, near-fault earthquakes are characterized by a short significant duration, and due to this the seismic energy input to the main structure occurs in a few seconds. This fact casts doubt on the TMD performance to control the structural response, as a result of the limited time in which the device can absorb energy from the main structure. The TMD effectiveness in structures subjected

*Corresponding author, Professor
E-mail: dambrosini@uncu.edu.ar

^a Dr. Eng.

^b Dr. Eng. Professor

to near-fault earthquakes has been studied to a lesser extent (Matta 2011, 2013, Nigdeli and Bekdas 2013). An analysis of the linear response of structures with TMD under near fault earthquakes was performed by Matta (2011). The author compared five optimization criteria and showed that a TMD with mass ratios of 50% can control the structural response in an effective and robust manner. In a later work by the same author (Matta 2013), the effect of near-fault earthquakes on the TMD performance was analyzed, representing earthquakes by pulse loads. In order to reduce the value of maximum displacement of the structure, a new optimization of the TMD parameters was proposed as function of the characteristics of the pulse used as excitation. When the optimum values obtained with this objective are compared with the optimum values that minimize the peak frequency response, it is observed that the optimum frequency ratio and especially the optimum damping are significantly lower compared to the case of harmonic loads. It is concluded that the proposed optimization is more efficient than classical optimization when trying to reduce the peak displacement in flexible structures by adding a TMD with large mass ratio. Quaranta *et al.* (2016) studied the performance of linear TMD in inelastic structures under pulse-like ground motions, using relatively large mass ratios. From the results of this study it was observed that the use of TMD with optimum values based on the elastic properties of the structure are not effective for displacement control when the structural response is nonlinear, becoming harmful an increase in the mass of the device. It is noteworthy that all of these previous studies lack of a nonlinear dynamic model needed to study the effect of TMD in structures that suffer degradation of stiffness and strength, reaching structural collapse against this type of action.

This paper evaluates the TMD performance in nonlinear reinforced concrete structures under near-fault earthquakes. With this purpose, full nonlinear numerical studies were carried out. Two structures with different fundamental periods and the same structural typology were studied. TMDs with three different mass ratio values, between 1 and 5%, were added on the structures analyzed. The nonlinear dynamic response of the numerical models subjected to five near-fault seismic records was studied. These records were selected based on their frequency content, which is close to the fundamental frequency of the structures. Due to this, the potential damage of the structures subjected to this set of seismic records is high. In order to establish the benefit produced by the use of TMD, the minimum amplitude of the seismic records that causes structural collapse was found and the results of the numerical models with and without the control device were compared. In previous papers by the authors (Domizio *et al.* 2015a, Domizio *et al.* 2015b), the effectiveness of TMDs in reducing the likelihood of structural collapse of steel structures was demonstrated for different cases. In this paper, the main question to be answered is: Is it possible, in the case of RC structures subjected to near-fault earthquakes, to reduce the likelihood of collapse using classical TMDs?. It is clear that the case of RC structures is very different from the case of steel structures, due to the greater stiffness degradation of the first ones. It is a real challenge, in the present state of the art of this topic, to perform full nonlinear numerical studies until collapse of RC structures.

Table 1 Structural element dimensions

Structure	Story	Beams Dimensions	Columns Dimensions
Three-story	1	25 x 50 cm	50 x 50 cm
	2	25 x 50 cm	50 x 50 cm
	3	25 x 30 cm	50 x 50 cm
Ten-story	1-4	25 x 70 cm	70 x 70 cm
	5-7	25 x 60 cm	60 x 60 cm
	8-10	25 x 50 cm	50 x 50 cm

Then, the novelty of the paper is to determine the TMD effectiveness in RC structures subjected to near fault earthquakes, by using a full nonlinear 3D model until collapse.

2. Description of the analyzed structures

The structures analyzed in this study consist of RC frames in the two main directions. The spatial arrangement of the structural elements can be observed in Fig. 1, while its dimensions are summarized in Table 1. These structures were designed according to Argentinean building codes from the early 1980s, i.e. Reglamento CIRSOC 201(1982) and NAA-80 (INPRES 1980), since the aim of this paper is to study the TMD performance on structures that require to be adapted to current seismic codes provisions. Details of the structural design were presented by Domizio (2016). The two analyzed structures have the same structural typology and different number of stories, 3 stories in the case of the first structure and 10 stories in the case of the second structure, with a typical story height of 2.65 m in both cases. Different numbers of stories were defined in each structure in order to assess the TMD effectiveness on two structures with different fundamental periods, which are representative of existing structures in high seismicity regions of Argentina.

2.1 Numerical models

In order to represent the nonlinear dynamic behavior of the analyzed structures, numerical models were developed with LS-DYNA software (Hallquist 2006). The RC modeling strategy used in this study was previously calibrated against experimental results (Domizio *et al.* 2017). Hexahedral solid finite elements with a single integration point were used in order to model the concrete, and the finite element mesh shown in Fig. 2 was generated. Considering the symmetry conditions, only a half of the structure was modeled. The Winfrith concrete model (Broadhouse and Neilson 1987) was used to represent the nonlinear concrete behavior. This material model was developed in order to study the effect of impact loads on reinforced concrete structures in the nuclear industry. The selected material model uses the shear failure surface proposed by Ottosen (1977), which takes into account the influence of confinement effect and deviatoric stress tensor on the material failure.

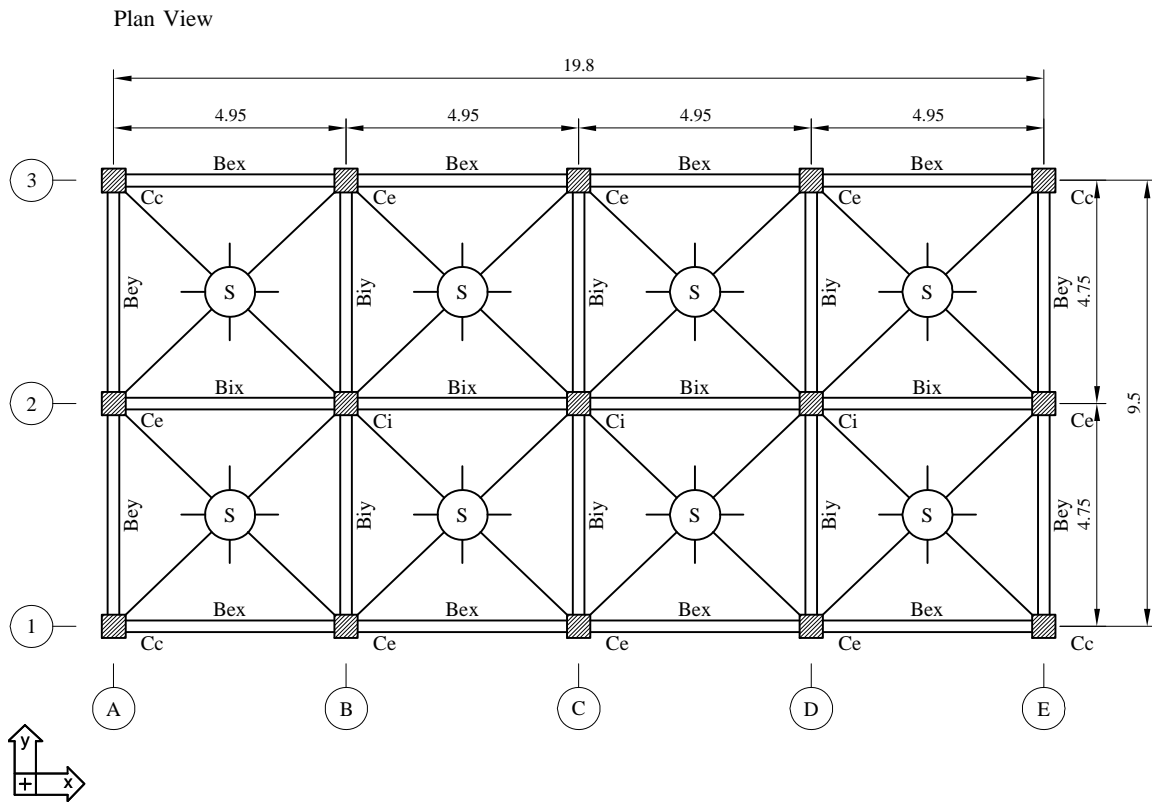


Fig. 1 Typical story plan

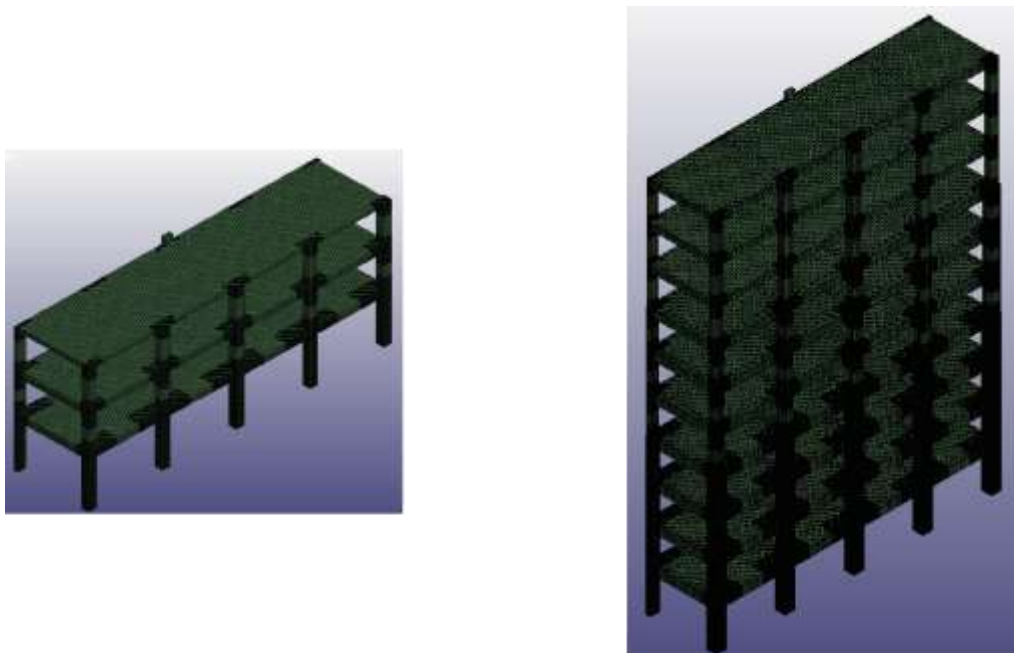


Fig. 2 General view of the finite element meshes

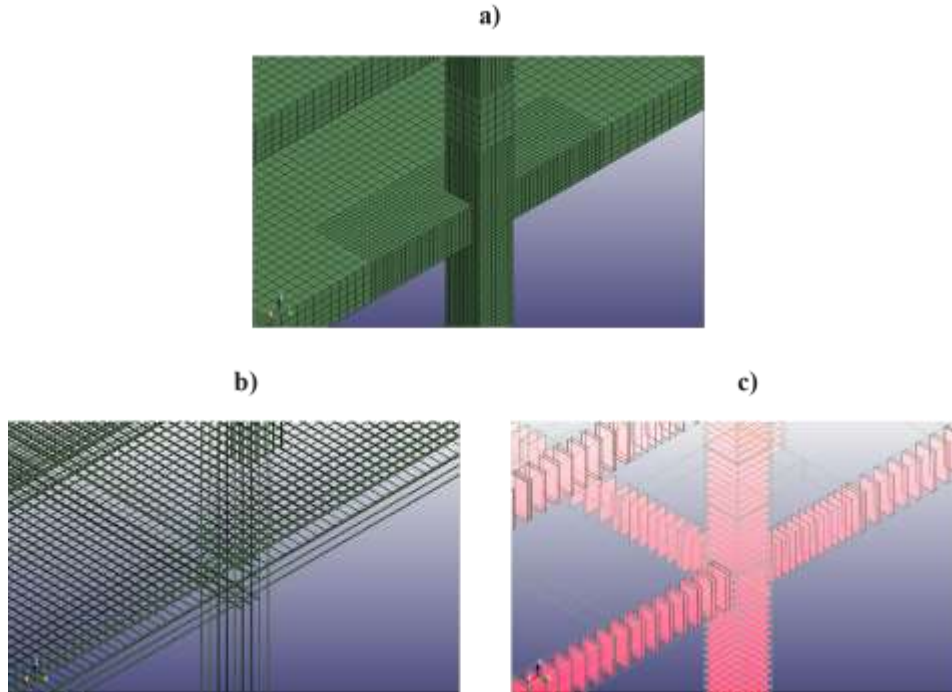


Fig. 3 Details of the finite element model: (a) mesh refinement at lower stories, (b) longitudinal reinforcement and (c) transverse reinforcement

The failure surface defined by Ottosen has four parameters that define its shape in the principal stress space. In the Winfrith concrete model, the four parameters of the failure surface are defined in terms of two material properties, which are the unconfined compressive and the tensile strength. Through the compression strength and the elastic modulus of concrete, the model provides the compaction curve relating the pressure and the volumetric strain. The material model is also able to represent the cracking of concrete under tensile stress, with a shear transfer through the crack surface that depends on the aggregate size defined in the material properties. Once the crack starts to propagate, normal and shear stresses decay linearly with the crack opening. An erosion algorithm based on a maximum effective strain criterion was used in order to avoid blocking problems and significant reductions of time step size caused by a large distortion of the solid finite element mesh.

The longitudinal reinforcement of the structural members was modeled with truss elements that support only axial forces (Fig. 3(b)). The mesh of these reinforcement elements shared nodes with solid elements mesh that represents concrete. A material model with a bilinear stress-strain relationship and kinematic hardening was used in the reinforcing elements. Meanwhile, the transverse reinforcement was modeled with a smeared approach over solid elements. This reinforcement is defined by the position of the layer where the steel bars are located (Fig. 3.c), and by the ratio of reinforcement cross-section to the solid element cross-sectional area. A material model with the same properties as in the case of longitudinal reinforcement was defined for the transverse reinforcement. The material properties used for the numerical simulation are presented in Table 2 and 3.

Table 2 Concrete material properties

Property	Adopted Value
Elastic modulus (GPa)	23
Poisson's ratio	0.18
Uniaxial compressive strength (MPa)	24
Uniaxial tensile strength (MPa)	2.4
Crack width at which crack-normal tensile stress goes to zero (mm)	0.02
Aggregate size (m)	0.025

Table 3 Steel material properties

Property	Adopted Value
Elastic modulus (GPa)	210
Poisson's ratio	0.30
Yield Stress (MPa)	420
Tangent Modulus (GPa)	10.5

On the other hand, the TMD was modeled as a rigid mass connected to the structure by a discrete element. This discrete element represents the response of the TMD spring and damper, arranged in parallel. A kinematic restriction was imposed on the displacement of the TMD mass so that the relative displacement between the control device and the main structure is one-directional, oriented with global X-X direction. Dynamic analyses were performed in this study with seismic loading only in X-X direction.

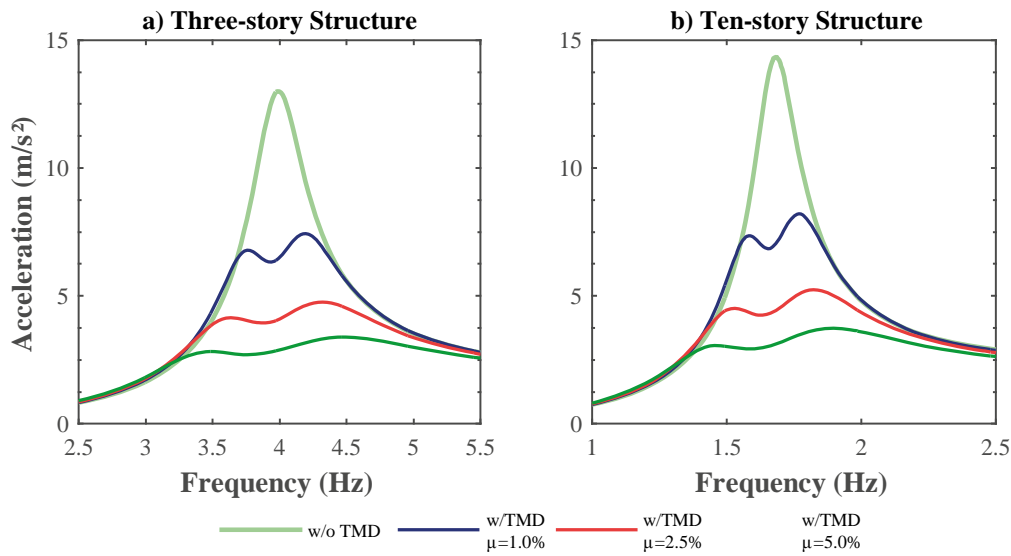


Fig. 4 Frequency response of the structures with and without TMD

Table 4 TMD parameters

Structure	Mass Ratio μ (adim.)	Optimal Parameters		TMD Mass (kg)	Spring Constant k (N/m)	Viscous Damping c (N.s/m)
		α_{opt} (adim.)	ζ_{opt} (adim.)			
Three-story	0,0100	0,988	0,061	2213	1,35E+06	6,67E+03
	0,0250	0,969	0,096	5533	3,24E+06	2,58E+04
	0,0500	0,940	0,135	11066	6,10E+06	7,03E+04
Ten-story	0,0100	0,988	0,061	7063	7,62E+06	8,96E+03
	0,0250	0,969	0,096	17659	1,84E+06	3,47E+04
	0,0500	0,940	0,135	35318	3,45E+06	9,45E+04

Based on the results of the mesh sensitivity analysis presented by Domizio (2016), the mesh was refined in columns and beams ends at lower stories of both structure. An element size of 6.25 cm was defined in these areas, which allows representing the behavior of the structural elements with 8 elements along the smaller dimension of the cross section. An element size of 12.5 cm was gradually used on upper stories, leading to a model with 196,926 nodes in the three-story structure and 960,150 nodes in the ten-story structure.

An explicit time integration scheme was used in this study, since the nonlinearity of concrete structures leads to severe convergence problems when implicit methods are employed. In this explicit integration scheme the time step is defined by the smaller element size of the model mesh, as well as the speed of sound in the material, which is a function of its density and stiffness.

The parameters that define the TMD response are: the mass ratio (μ) between the TMD mass and the mass of the structure; the frequency ratio (α) between the TMD frequency and the frequency of the structure; and the damping ratio (ζ) of the device. In order to define the parameters of frequency and damping ratio, the following

expressions of optimal values, given by Warburton (1982) for the case of harmonic base excitation, were employed.

$$\alpha_{opt} = \frac{\sqrt{1 - \frac{\mu}{2}}}{1 + \mu} \tag{1}$$

$$\zeta_{opt} = \frac{\sqrt{3 \cdot \mu}}{\sqrt{8 \cdot (1 + \mu) \cdot \left(1 - \frac{\mu}{2}\right)}} \tag{2}$$

The mass of the structure was characterized by the modal mass obtained normalizing the eigenvector of the first mode with a unit value at the level where the TMD was located. From a modal analysis on the numerical model of the three-story structure, a frequency of 3.975 Hz was obtained for the fundamental mode in the X-X direction with a modal mass of 221 t. In the case of the ten-story structure, the frequency of the fundamental mode was found to be of 1.674 Hz with a modal mass of 706 t. The TMD parameters values adopted, according to the three mass ratio values employed in this study, are summarized in Table 4.

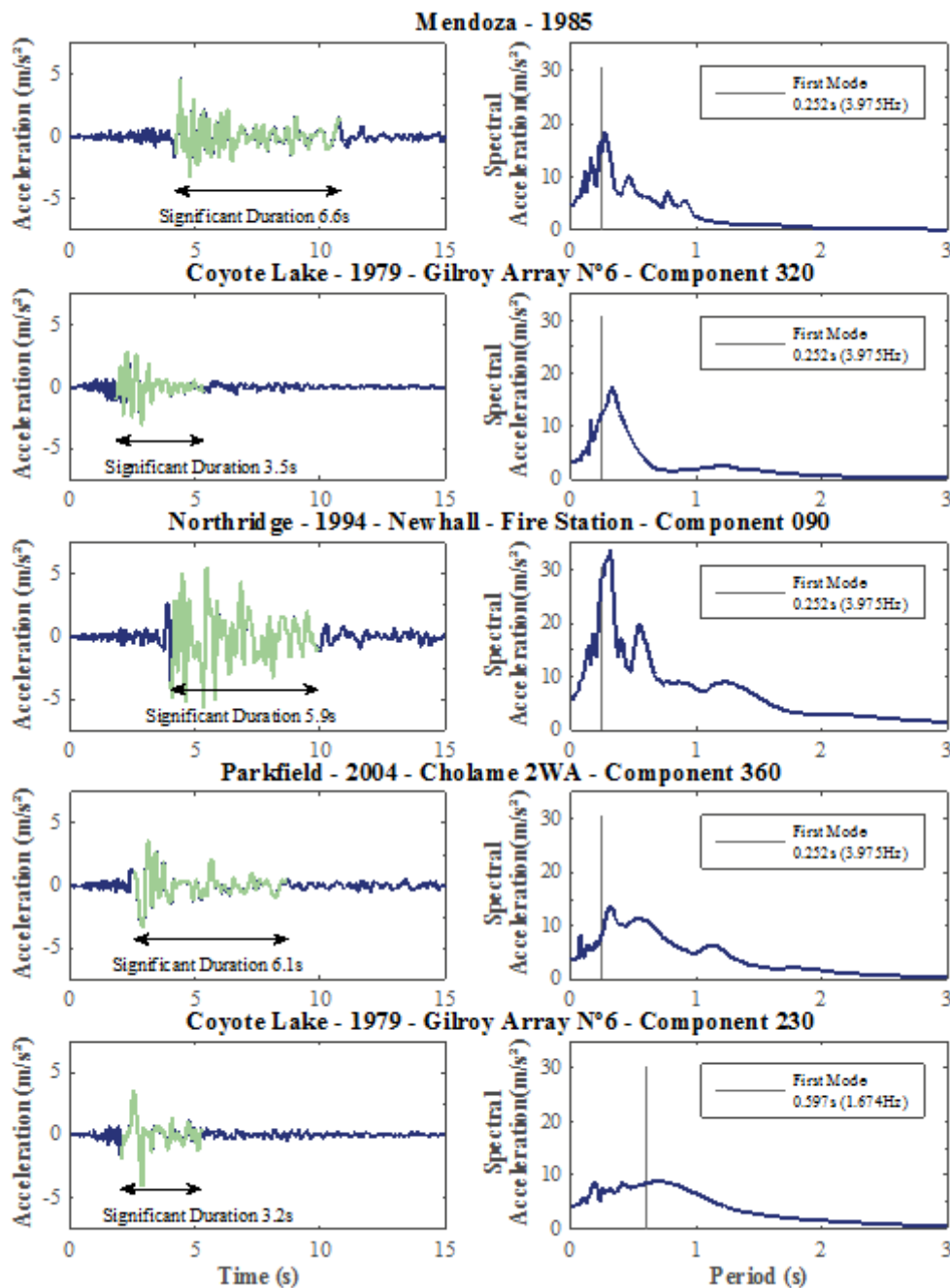


Fig. 5 Acceleration records and response spectrum of the selected seismic records

The frequency response in terms of acceleration on the top story when a unit acceleration is applied at the base of the structures can be observed in Fig. 4.

2.2 Seismic records

Seismic records used in this study were selected to represent the effect of near-fault earthquakes on the analyzed structures. The characteristics of the selected records are summarized in Table 5. The first four records were used in analyzing the three-story structure, while the fifth record was applied on the 10-story structure.

Acceleration records are presented in Fig. 5, where significant duration, according to the criteria established by Trifunac and Brady (1975), is highlighted. The response spectra of these seismic records can also be seen in Fig. 5 wherein the fundamental period of the analyzed structures is indicated.

It can be seen in Fig. 5 that acceleration records have a frequency content close to the fundamental period of the structures and consequently the selected seismic records have a high destructive potential on these structures.

Table 5 Near-fault seismic records selected

Event	Year	Moment Magnitude	Station	Component	Peak Ground Acceleration (m/s ²)
Mendoza, Argentina	1985	6,3	--	--	4,68
Coyote Lake, U.S.A (1)	1979	5,7	Gilroy Array N%	320	3,12
Northridge, U.S.A (1)	1994	6,7	Newhall Fire Station	090	5,72
Parkfield, U.S.A (1)	2004	6,0	Cholame 2WA	360	3,66
Coyote Lake, U.S.A (1)	1979	5,7	Gilroy Array N%	230	4,13

Source: (1) Peer Ground motion Database (<http://ngawest2.berkeley.edu/>)

Table 6 Collapse acceleration of structures without TMD

Event	Year	Station	Component	Structure	Collapse Acceleration (m/s ²)
Mendoza	1985	--	--		21,03
Coyote Lake	1979	Gilroy Array N%	320	Three-story	31,39
Northridge	1994	Newhall Fire Station	090		13,68
Parkfield	2004	Cholame 2WA	360		15,20
Coyote Lake	1979	Gilroy Array N%	230	Ten-story	18,07

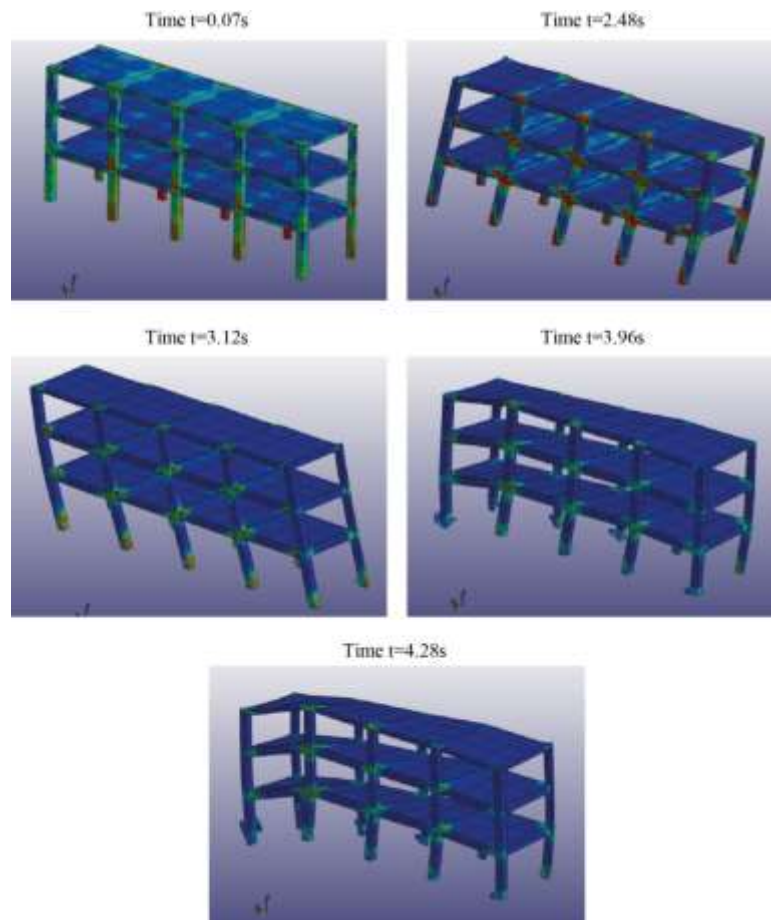


Fig. 6 Effective strain and collapse mechanism caused by Coyote Lake seismic record

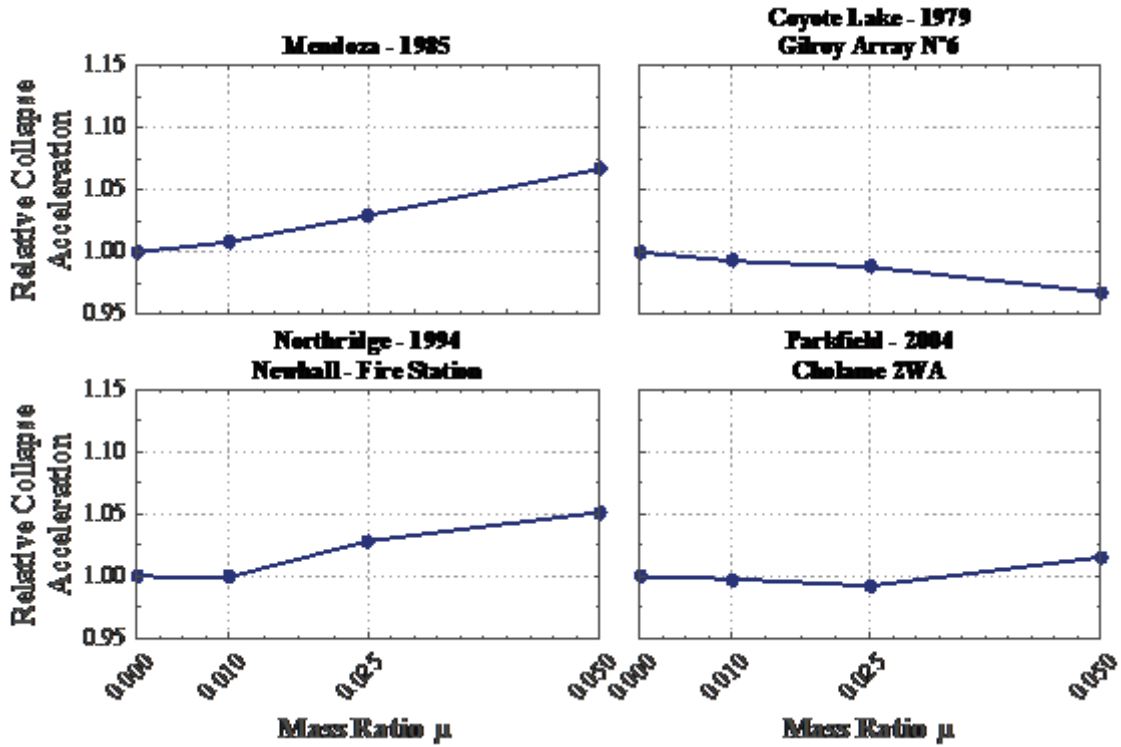


Fig. 7 Collapse acceleration of the three-story structure with TMD relative to the uncontrolled case

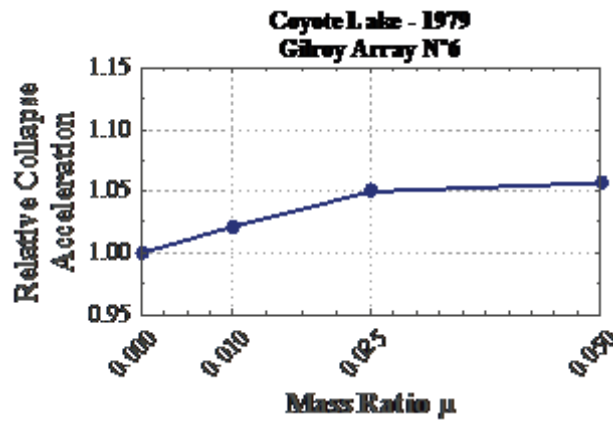


Fig. 8 Collapse acceleration of the ten-story structure with TMD relative to the uncontrolled case

3. Collapse acceleration analysis

The minimum amplitude of the peak ground accelerations (PGA) of each acceleration record that cause the collapse of the structure, called collapse acceleration, with and without TMD was found scaling records by the bisection method, as detailed by Domizio (2015a).

Table 6 summarizes the PGA of each seismic record that causes the collapse of the structure without the addition of TMD.

The formation of the collapse mechanism in the three-story structure without the TMD addition under Coyote Lake seismic record, scaled to the amplitude of collapse acceleration, is presented in Fig. 6. Displacements have

been magnified 5 times for better visualization. This figure shows the effective strain in the structure, which is the base of the erosion criteria adopted in the numerical model. It can be seen in these figures how the highest strains are located mainly at the first story beam-column joints and at the first story columns base, where finally the shear failure takes place.

Collapse accelerations of the structure obtained from analyzes where the TMD was included as vibration control device are presented in Figs. 7 and 8 for the case of the structures of three and ten stories respectively. Results are expressed relative to the structural response without control, where the mass assigned to TMD is considered to be zero. It can be seen that the increase in collapse acceleration due to

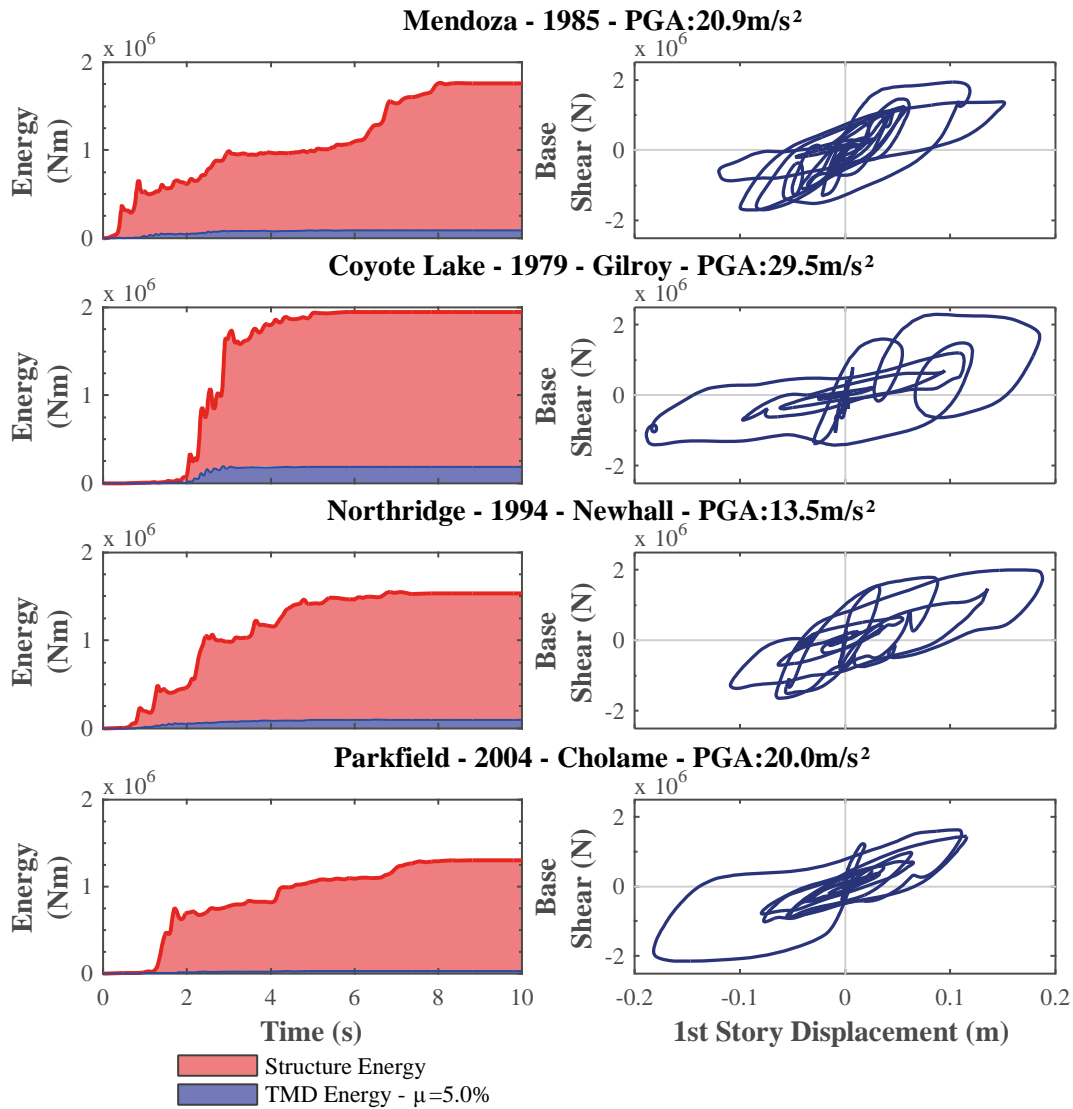


Fig. 9 Energy provided by the seismic action to the main structure and base shear as function of first story displacement at the three-story structure

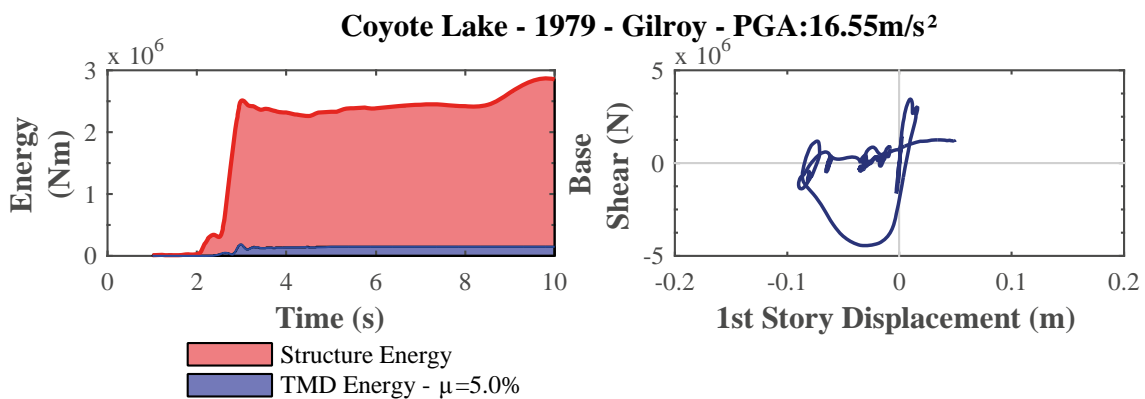


Fig. 10 Energy provided by the seismic action to the main structure and base shear as function of first story displacement at the ten-story structure

incorporation of the TMD did not exceeded 7% compared to the case without control in both structures. As can be seen in Fig. 7, the addition of a TMD was even harmful on the three-story structure under the action of Coyote Lake seismic record, with an almost linear decrease in collapse acceleration as the amount of mass assigned to the device was increased. In all other cases, the increase in TMD mass led to a slight increase of the collapse acceleration.

Observations on the TMD performance to prevent the collapse of the reinforced concrete structures analyzed can be confirmed in Figs. 9 and 10. In these figures the total seismic energy provided to the main structure by each seismic record and the amount of energy transferred to the TMD ($\mu = 5\%$) are shown. It can also be observed in the figures, the base shear - first story displacement relationship. The seismic records were scaled in this case slightly under the collapse acceleration; this is the maximum record amplitude that the structure can support without collapsing.

In all cases it can be seen how the energy is dissipated mostly in plastic strains and degradation of the main structure, with significantly less energy that can be absorbed by the TMD. This energy transfer to the control device occurs after the sudden increases of the structure energy, which take place at the beginning of the significant duration of the seismic action.

Another important factor in the low TMD effectiveness is the detuning effect. This effect occurs in this case as a result of stiffness degradation that the structure undergoes through the successive vibration cycles, as shown in Figs. 9 and 10.

4. Conclusions

In this paper, the TMD performance to control the nonlinear dynamic response to collapse of reinforced concrete structures subjected to near-fault earthquake was studied. The effect of the control device on the structure was determined from nonlinear dynamic analysis performed on a finite element model. Two reinforced concrete frames, with three and ten stories, were analyzed. TMD with three different mass values were added to the structures, representing 1%, 2.5% and 5% of the modal mass of the structure. The frequency and damping ratio of the TMD were defined according to a classic expression of optimal values for harmonic actions applied at the base of the structure. For the three-story structure 4 near-fault seismic records were selected, and a single record was used in the ten-story structure. These seismic records were selected for having frequency content close to the fundamental frequencies of the analyzed structures.

In order to quantify the benefits produced by the added control device, the smaller amplitude of each seismic record that causes structural collapse was sought. This collapse acceleration was initially found for the case of the structure without TMD. The analysis was repeated for the model of the structure with the addition of the device, obtaining increases in terms of collapse acceleration that did not exceed 7% compared to uncontrolled case in both

structures. In the case of Coyote Lake seismic, the addition of TMD in the three-story structure could be even harmful, reducing the maximum acceleration that supports the structure without collapsing. The relatively low increase in the collapse acceleration was verified through the results in terms of the seismic energy supplied to the structure. Based on these results, it can be seen that most of the energy of the seismic action was dissipated in plastic strains and damage on the reinforced concrete structure rather than being transferred to the control device. Another reason for the low performance of the device was observed from the analysis of the base shear as function of displacement at the first story. It can be seen that, in all cases studied in this paper, seismic records scaled to the collapse acceleration level caused high stiffness degradation, leading to the detrimental detuning effect and the consequent decrease in the effectiveness of the device.

This drawback of detuning could be partially overcome using multiple TMDs with decreasing frequency ratios. Other option could be the use of semiactive TMDs (Sun and Nagarajaiah 2014; Sun *et al.* 2018), which allows the stiffness and damping of the TMD to vary with the time.

Acknowledgments

The financial support of CONICET and the National University of Cuyo is gratefully acknowledged. Special acknowledgements are extended to the reviewers of the first version of the article because his/her useful suggestions led to improvements of the work.

References

- Broadhouse, B.J. and Neilson, A.J. (1987), "Modelling reinforced concrete structures in DYNA3D", *Rep. AEEW-M2465, UK At. Energy Authority, Winfrith*.
- Cheng, C.T. and Chen, F.L. (2014), "Seismic performance of a rocking bridge pier substructure with frictional hinge dampers", *Smart Struct. Syst.*, **14**(4), 501-516. <http://dx.doi.org/10.12989/sss.2014.14.4.501>.
- Choi, E. *et al.* (2017), "Cyclic compressive behavior of polyurethane rubber springs for smart dampers", *Smart Struct. Syst.*, **20**(6), 739-757. <https://doi.org/10.12989/sss.2017.20.6.739>.
- CIRSOC (1982), "Reglamento CIRSOC 201: Proyecto, Cálculo y Ejecución de Estructuras de Hormigón Armado y Pretensado" Centro de Investigación de los Reglamentos Nacionales de Seguridad para las Obras Civiles
- Daniel, Y. and Lavan, O. (2013), "Allocation and sizing of multiple tuned mass dampers for seismic control of irregular structures", In, *Geotechnical, Geological and Earthquake Engineering.*, 323-338.
- Domizio, M. (2016), "Effectiveness analysis of tuned mass damper against structural collapse due to near fault earthquakes", PhD Thesis (in Spanish). 2016.
- Domizio, M. *et al.* (2017), "Nonlinear dynamic numerical analysis of a RC frame subjected to seismic loading", *Eng. Struct.*, **138**, 410-424. <https://doi.org/10.1016/j.engstruct.2017.02.031>.
- Domizio, M. *et al.* (2015), "Performance of TMDs on nonlinear structures subjected to near-fault earthquakes", *Smart Struct. Syst.*, **16**(4), 725-742.

- <http://dx.doi.org/10.12989/sss.2015.16.4.725>.
- Domizio, M. *et al.* (2015), "Performance of tuned mass damper against structural collapse due to near fault earthquakes", *J. Sound Vib.*, **336**, 32-45. <https://doi.org/10.1016/j.jsv.2014.10.007>.
- Elias, S. *et al.* (2017), "Distributed tuned mass dampers for Multi-mode control of benchmark building under seismic excitations", *J. Earthq. Eng.*, **2469**, 1-36. <https://doi.org/10.1080/13632469.2017.1351407>.
- Engle, T. *et al.* (2015), "Hybrid tuned mass damper and isolation floor slab system optimized for vibration control", *J. Earthq. Eng.*, **19**(8), 1197-1221. <https://doi.org/10.1080/13632469.2015.1037406>.
- Fadel Miguel, L.F. *et al.* (2016), "A novel approach to the optimum design of MTMDs under seismic excitations", *Struct. Control Heal. Monit.*, **23**(11), 1290-1313. <https://doi.org/10.1002/stc.1845>.
- Greco, R. *et al.* (2014), "Robust design of tuned mass dampers installed on multi-degree-of-freedom structures subjected to seismic action", *Eng. Optim.*, **47**(8), 1-22. <https://doi.org/10.1080/0305215X.2014.941288>.
- Hallquist, J.O. (2006), "LS-DYNA theory manual"
- Hoang, T. *et al.* (2016), "Structural impact mitigation of bridge piers using tuned mass damper", *Eng. Struct.*, **112**, 287-294. <https://doi.org/10.1016/j.engstruct.2015.12.041>.
- Hsiao, P.-C. *et al.* (2016), "Development and testing of naturally buckling steel braces", *J. Struct. Eng.*, **142**(1), 4015077. [https://doi.org/10.1061/\(ASCE\)ST.1943-541X.0001319](https://doi.org/10.1061/(ASCE)ST.1943-541X.0001319).
- INPRES (1980), "Normas Antisísmicas Argentinas NAA-80" Instituto Nacional de Prevención Sísmica.
- Jiang, Q. *et al.* (2014), "Shaking table model test and FE analysis of a reinforced concrete mega-frame structure with tuned mass dampers", *Struct. Des. Tall Spec. Build.*, **23**(18), 1426-1442. <https://doi.org/10.1002/tal.1150>.
- Jimenez-Alonso, J.F. and Saez, A. (2018), "Motion-based design of TMD for vibrating footbridges under uncertainty conditions", *Smart Struct. Syst.*, **21**(6), 727-740. <https://doi.org/10.12989/sss.2018.21.6.727>.
- Lin, G.-L. *et al.* (2015), "Vibration control performance of tuned mass dampers with resettable variable stiffness", *Eng. Struct.*, **83**, 187-197. <https://doi.org/10.1016/j.engstruct.2014.10.041>.
- Losanno, D. *et al.* (2017), "Design and retrofit of multistory frames with elastic-deformable viscous damping braces", *J. Earthq. Eng.*, 1-24. <https://doi.org/10.1080/13632469.2017.1387193>.
- Lu, Z. *et al.* (2016), "An experimental study of vibration control of wind-excited high-rise buildings using particle tuned mass dampers", *Smart Struct. Syst.*, **18**(1), 93-115. <https://doi.org/10.12989/sss.2016.18.1.093>.
- Lu, Z. *et al.* (2017), "Experimental and analytical study on the performance of particle tuned mass dampers under seismic excitation", *Earthq. Eng. Struct. D.*, **46**(5), 697-714. <https://doi.org/10.1002/eqe.2826>.
- Matta, E. (2013), "Effectiveness of tuned mass dampers against ground motion pulses", *J. Struct. Eng.*, **139**(2), 188-198. [https://doi.org/10.1061/\(ASCE\)ST.1943-541X.0000629](https://doi.org/10.1061/(ASCE)ST.1943-541X.0000629).
- Matta, E. (2011), "Performance of tuned mass dampers against near-field earthquakes", *Struct. Eng. Mech.*, **39**(5), 621-642. <https://doi.org/10.12989/sem.2011.39.5.621>.
- Miranda, J.C. (2013), "A method for tuning tuned mass dampers for seismic applications", *Earthq. Eng. Structural D.*, **42**(7), 1103-1110. <https://doi.org/10.1002/eqe.2271>.
- Nigdeli, S.M. and Bekdas, G. (2013), "The effect of impulsive motions on optimum tuned mass damper parameters", *Proceedings of the 11th International Conference on Vibration Problems.*, 2-10.
- Niu, H. *et al.* (2018), "Mitigation of wind-induced vibrations of bridge hangers using tuned mass dampers with eddy current damping", *Smart Struct. Syst.*, **22**(6), 727-741. <https://doi.org/10.12989/sss.2018.22.6.727>.
- Ottosen, N.S. (1977), "A failure criterion for concrete", *J. Eng. Mech.*, 527-535.
- Pisal, A.Y. and Jangid, R.S. (2016), "Vibration control of bridge subjected to multi-axle vehicle using multiple tuned mass friction dampers", *Int. J. Adv. Struct. Eng.*, **8**(2), 213-227.
- Quaranta, G. *et al.* (2016), "Effectiveness of design procedures for linear TMD installed on inelastic structures under pulse-like ground motion", *Earthq. Struct.*, **10**(1), 239-260. <https://doi.org/10.12989/eas.2016.10.1.239>.
- Rakicevic, Z.T. *et al.* (2012), "Effectiveness of tune mass damper in the reduction of the seismic response of the structure", *Bull. Earthq. Eng.*, **10**(3), 1049-1073.
- Salvi, J. and Rizzi, E. (2016), "Closed-form optimum tuning formulas for passive Tuned Mass Dampers under benchmark excitations", *Smart Struct. Syst.*, **17**(2), 231-256. <http://dx.doi.org/10.12989/sss.2016.17.2.231>.
- Shen, S. *et al.* (2017), "Development of a double-sliding friction damper (DSFD)", *Smart Struct. Syst.*, **20**(2), 151-162. <https://doi.org/10.12989/sss.2017.20.2.151>.
- Sun, C. and Nagarajaiah, S. (2014), "Study on semi-active tuned mass damper with variable damping and stiffness under seismic excitations", *Struct. Control Health. Monit.*, **21**(6), 890-906. <https://doi.org/10.1002/stc.1620>.
- Sun, S. *et al.* (2018), "Development of magnetorheological elastomers-based tuned mass damper for building protection from seismic events", *J. Intel. Mat. Syst. Str.*, **29**(8), 1777-1789. <https://doi.org/10.1177/1045389X17754265>.
- Trifunac, M. and Brady, A.G. (1975), "A study on the duration of strong earthquake ground motion", *Bull. Seismol. Soc. Am.*, **65**, 581-626.
- Warburton, G.B. (1982), "Optimal absorber parameters for various combinations of response and excitation parameters", *Earthq. Eng. Struct. D.*, **10**(3), 381-402. <https://doi.org/10.1002/eqe.4290100304>.
- Yu, Y.-J. *et al.* (2010), "Analytical studies of a full-scale steel building shaken to collapse", *Eng. Struct.*, **32**(10), 3418-3430. <https://doi.org/10.1016/j.engstruct.2010.07.015>.

FC

